Avestia Publishing
Journal of Biomedical Engineering and Biosciences (JBEB)
Volume 11, Year 2024
ISSN: 2564-4998
DOI: 10.11159/jbeb.2024.002

Analysis of Morphology, Hemodynamics and Structural Mechanics for the Establishment of Growth History of Cerebral Aneurysm

Jozsef Nagy[1], Julia Maier[2], Wolfgang Fenz[3], Zoltan Major[2], Andreas Gruber[4], Matthias Gmeiner[4]
[1]eulerian-solutions e.U.
Leonfeldnerstraße 245, Linz, Austria
jozsef.nagy@eulrian.solutions.com
[2]Johannes Kepler University Linz - Institute of Polymer Product Engineering
Altenberger Strasse 69, Linz, Austria
julia.maier@jku.at; zoltan.major@jku.at
[3]RISC Software GmbH
Softwarepark 32a, Hagenberg, Austria
wolfgang.fenz@risc-software.at
[4]Johannes Kepler University Linz - Universitätsklinik für Neurochirurgie
Wagner-Jauregg-Weg 15, Linz, Austria
andreas.gruber_1@kepleruniklinikum.at; matthias.gmeiner@kepleruniklinikum.at

Abstract - *We analyzed the growth process of a single cerebral aneurysm using Fluid-Structure Interaction (FSI) simulations establishing a history including important events in morphology, hemodynamics as well as structural mechanics.*
Data of one patient was obtained between the years 2012 and 2022. The medical imaging data of these aneurysms was provided in the form of digital subtraction angiography, which was transformed into stereolithography format as geometry input. With the FSI simulations typical hemodynamic (wall shear stress, oscillatory shear index) and a structural mechanic quantity (Mises stress) were identified. With the addition of morphological parameters (Size, Volume, L2-norm of Gaussian curvature) significant changes can be found during the growth history of the selected aneurysm.
Wall shear stress is highest during aneurysm initiation, while decreasing during aneurysm growth. Oscillatory shear index increases over time especially in the region of strong aneurysm growth. Strong changes in geometry induce subsequent changes in hemodynamics. Wall stress remains constant throughout the growth period of the selected aneurysm. However, shortly before aneurysm rupture wall stress increases significantly.
Simulation results of aneurysm growth history can be utilized to identify important events of a growing aneurysm, enabling a better understanding of the behaviour as well as a better estimation for the best time for patient treatment.

Keywords**:** cerebral aneurysms, growth history, Fluid-Structure Interaction, aneurysm initiation, aneurysm rupture

© Copyright 2024 Authors - This is an Open Access article published under the Creative Commons Attribution License terms (http://creativecommons.org/licenses/by/3.0). Unrestricted use, distribution, and reproduction in any medium are permitted, provided the original work is properly cited.

1. Introduction

Cerebral aneurysms occur in approximately 2-5% of the general population [1]. Rupture of aneurysms leads to subarachnoid hemorrhage (SAH), which is usually associated with high mortality and morbidity. Several studies have highlighted different clinical, genetic, morphological or hemodynamic factors known in the development, growth and rupture of cerebral aneurysms [2-4].

The increasing utilization of medical imaging has led to the detection of a greater number of unruptured aneurysms. This, in turn, leads to a greater need for treatment decisions. Only aneurysms close to rupture should be treated, because the treatment itself carries many risks for the patient.

Date Received: 2024-01-12
Date Accepted: 2024-09-09
Date Published: 2024-09-16
Date Published: 2024-09-25

Therefore, reliable decision support is needed to better treat patients.

Multiple studies in literature using computational fluid dynamics (CFD) have been able to demonstrate significantly different hemodynamics between ruptured and unruptured aneurysms [5-7]. Hemodynamic phenomena provide mechanical triggers that translate into biological signals that lead to eventual aneurysm growth and rupture [8]. Hemodynamics is influenced by the geometry of the aneurysm, therefore also the morphological parameters [9].

Furthermore, although many detailed fluid dynamics simulations, including complex flow models, have already been performed [2,3,5-10], only a few have been done so far studies focused on structural dynamics calculations. [11,12]. Previously we published a comprehensive assessment of a method using fluid-structure interaction (FSI) analysis, which was validated with the help of an experimental setup [13]. In this work additional validation is presented in order to further guarantee the correctness of the results.

With this method it is possible to track the development of cerebral aneurysms and quantitatively analyze the change in aneurysm behaviour utilizing the medical imaging data from two subsequent routine examinations. In this work we present the full quantified evaluation of morphological, hemodynamic as well as structural mechanical quantities during the growth period of one aneurysm. We identify significant changes in parameters over the years indicating important events in growth history. These events can give neurosurgeons critical information about the risk of rupture.

2. Methods

2. 1. Patient image data and simulation geometry

The aneurysm geometry is extracted from medical image data obtained via digital subtraction angiography (DSA). Intensity thresholding and minor editing of the voxel volume is performed in the segmentation of the cerebral aneurysm geometry. This is converted into a surface mesh and inlet as well as outlet planes are placed. The final set of surfaces (vessel, aneurysm, inflow, outflow) is saved as STL files. The volumetric fluid mesh is automatically generated utilizing the STL files as input. The solid vessel wall mesh is extruded from the fluid mesh with a certain pre-defined thickness (0.2 mm).

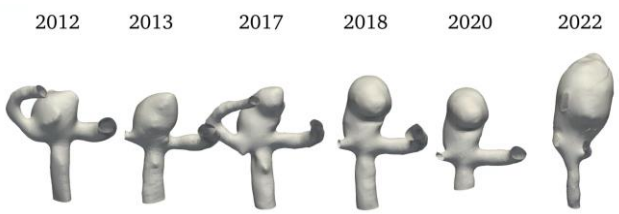

Figure 1: Geometries extracted from medical imaging data; date of data indicated in the top

For this study a set of medical imaging data of the same patient from the years 2012, 2013, 2017, 2018, 2020 and 2022 (see figure 1) is analyzed and changes in morphology, hemodynamic and structural mechanics identified. Before the image in 2022 SAH occurred in the aneurysm.

2. 2. Hemodynamic and structural mechanical modeling

An in-house finite volume solver [13] based on the open-source computational fluid dynamics tool OpenFOAM [14] in combination with the fluid-structure interaction library solids4Foam [15] was used to numerically solve the unsteady equations of the process.

For hemodynamic modelling the governing equations are given by the principles of mass and momentum conservation with the help of the continuity equation as well as the Navier Stokes equations,

$$\frac{\partial \rho}{\partial t} + \nabla \cdot \rho \mathbf{u} = 0 \tag{1}$$

$$\frac{\partial \rho \mathbf{u}}{\partial t} + \nabla \cdot \rho \mathbf{u}\mathbf{u} = -\nabla p + \boldsymbol{\nabla} \cdot \boldsymbol{\sigma} + \mathbf{F} \tag{2}$$

Here, ρ is the fluid density, t is the time, $\mathbf{u}$ is the velocity vector, p is the fluid pressure, $\boldsymbol{\sigma}$ is the fluid stress tensor and $\mathbf{F}$ is the vector of possibly additional forces (e.g. gravitation). In order to analyse hemodynamic results, the oscillatory shear index is defined as

$$\mathrm{OS}I = \frac{1}{2}\left(1 - \frac{\left\| \int_0^T \boldsymbol{\sigma}_\mathbf{W}\, dt \right\|}{\int_0^T \|\boldsymbol{\sigma}_\mathbf{W}\|\, dt}\right) \tag{3}$$

where, σ_s is the fluid wall shear stress (WSS) vector. The index is defined in the interval between [0;0.5] and gives the quantity of oscillatory behaviour of the wall shear stress on the fluid wall.

For structural mechanic modelling, the principle of force conservation is utilized. For linear elastic materials the equation is given by

$$\int_{\Omega_0} \frac{\partial^2 \rho_s \mathbf{u}_s}{\partial t^2} d\Omega_0 = \oint_{\Gamma_0} \mathbf{n_0} \cdot \boldsymbol{\sigma_s} d\Gamma_0 + \int_{\Omega_0} \rho_s \mathbf{b}\, d\Omega_0 \quad (4)$$

$$\boldsymbol{\sigma_s} = 2\mu\boldsymbol{\varepsilon_s} + \lambda\, tr(\boldsymbol{\varepsilon_s})\, I \quad (5)$$

$$\boldsymbol{\varepsilon_s} = \frac{1}{2}\left(\boldsymbol{\nabla}\mathbf{u}_s + \boldsymbol{\nabla}\mathbf{u}_s{}^T\right) \quad (6)$$

$$\mu = \frac{E}{2(1+\nu)} \quad (7)$$

$$\lambda = \frac{\nu E}{(1+\nu)(1-2\nu)} \quad (8)$$

Here, ρ_s is the solid density, $\mathbf{u}_s$ is the vector of displacement, $\mathbf{n_0}$ is the surface normal vector, $\boldsymbol{\sigma_s}$ is the solid stress tensor and $\mathbf{b}$ is the vector of possible body forces. E is Young's modulus and ν is Poisson's ratio.

Equations (1)-(8) are coupled iteratively in a Fluid-Structure Interaction method described in further detail in [13].

3. Additional validation data

In [13] an experimental setup for validation is presented including two pressure curves (trapezoidal and blood pressure curve from literature [17]) exhibited by a pump. The pressure change over time induces a certain strain in an elastic tube. This strain can be used to compare experiments and simulation. The elastic tube has a constant wall thickness in a set of experiments and varying wall thickness in a second set of experiments. In this work, results of strain induced by an additional sinusoidal pressure curve are presented. The remaining settings are utilized as reported in [13].

Figure 2 shows the results of simulation of the experimental setup and results in experiments. The green curves indicate the measured pressure curves in two separate experiments. There are differences in experiments due to inaccuracies in the experimental setup. The first pressure profile is used in the simulation as a pressure boundary condition. The two blue curves show the strain over time in the two experiments. In comparison, the orange curve of the simulation shows a good agreement in its time evolution, as it remains mostly in-between the two experimental curves. Similar behaviour can be seen in Figure 3 for varying wall thickness.

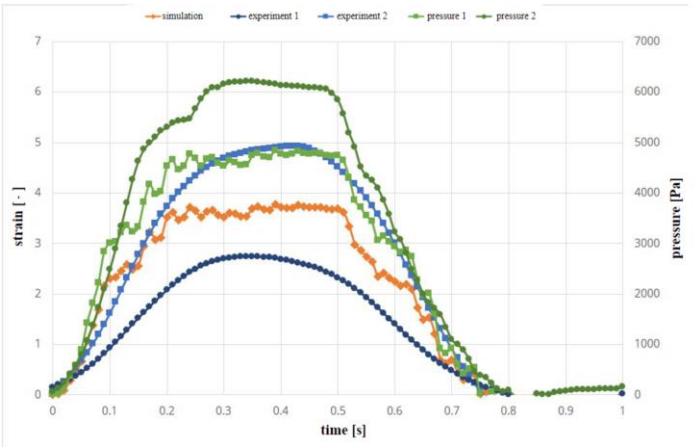

Figure 2. Sinusoidal pressure curves in the channel with constant wall thickness: strain curve (orange) in simulation; strain curves in two experiments (blue); pressure curves in two experiments (green)

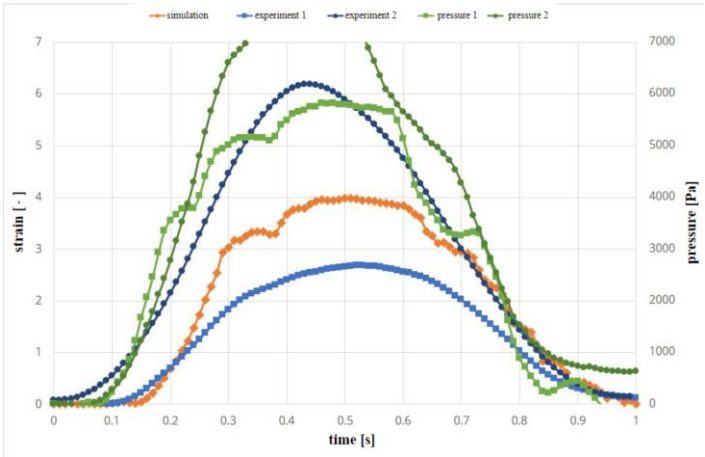

Figure 3. Sinusoidal pressure curves in the channel with varying wall thickness: strain curve (orange) in simulation; strain curves in two experiments (blue); pressure curves in two experiments (green)

Table 1 shows the values of strain in the elastic channels induced by the time dependent pressure curve evaluated at the time of maximum pressure. Both in case of constant and varying wall thickness the strain values

are in-between those measured in experiments (2.76%<**3.82%**<4.93%; 2.62%<**3.94%**<6.17%).

Table 1. Strain value in experiments and simulation at time of maximum pressure.

wall thickness	simulation [%]	experiment 1 [%]	experiment 2 [%]
constant	3.82	4.93	2.76
varying	3.94	2.62	6.17

Similar to [13], results in this work of the sinusoidal pressure curve indicate that the difference between experiment and simulation is in the same order of magnitude as the difference between two experimental runs.

4. Results and discussion

For the aneurysm initiation and growth process, the role of the wall shear stress as well as OSI has recently been discussed with divergent results [3,16]. Typically, they show an inverse behaviour during aneurysm growth, while one is increasing, the other is decreasing. Some studies [11,12] incorporate structural mechanic analysis into the behaviour of aneurysms, however these mostly concentrate on abdominal aneurysms. According to the knowledge of the authors, almost no work was done on the structural mechanic analysis of cerebral aneurysms.

For best visualization wall shear stress will be shown in an interval between 0 and 1 Pa, OSI between 0 and 0.25 and the Mises stress of the vessel wall between 0 and 1.2 kPa.

Figure 4 (a) shows the change in wall shear stress (WSS) in Pa over the years. During the first year a significant region with high WSS values can be identified. This correlates to the initiation process of the aneurysm as described in [3,16]. WSS gradually is being reduced in the aneurysm during the growth process. Figure 4 (b) shows the development of OSI in the aneurysm. While being comparatively low during the initiation process, a clear region of increased OSI can be identified in the direction of growth during the years. Figure 4 (c) shows the Mises stress in the vessel wall. No significant qualitative change can be identified especially in the early stages of the growth, which implies that aneurysm growth in the initial stages did not change the stress on the vessel tissue.

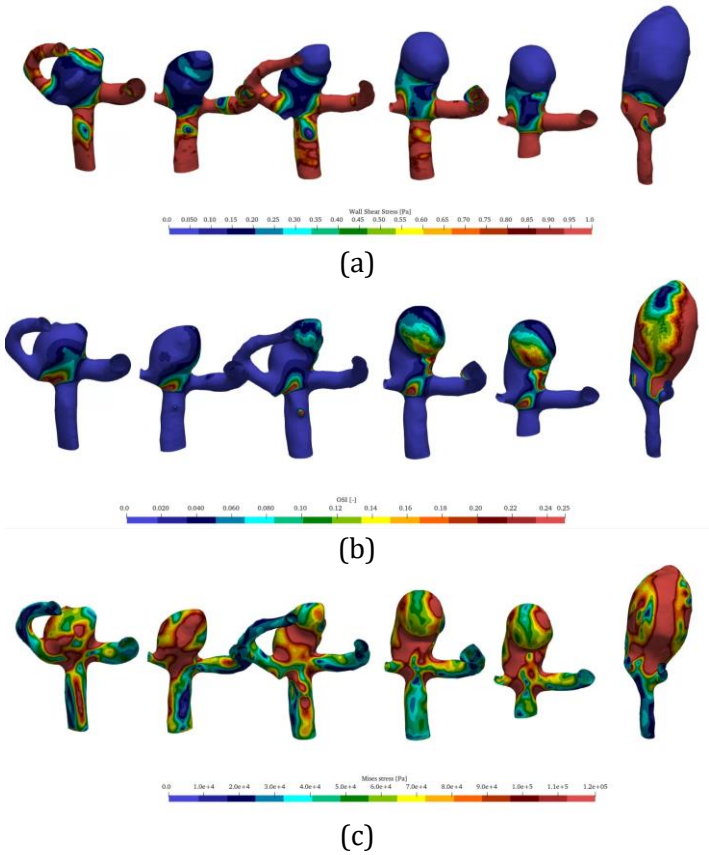

(a)

(b)

(c)

Figure 4: Wall shear stress (a), oscillatory shear index (OSI; b) and Mises stress (c) in the investigated geometries

Table 2 shows the investigated parameters (morphologic: Size S, Volume V, L2 norm of Gaussian curvature; hemodynamic: average WSS and average OSI; structural mechanic: average Mises stress). Here, the average values are taken only from the aneurysm, not the parent vessel. Additionally, the evaluation of maximum values is omitted as they are restricted to local positions in the aneurysm and are not adequate for analyzing the overall behaviour of the aneurysm.

Table 2: Change in typical parameters of the investigated aneurysm over the years

Parameter	2012	2013	2017	2018	2020	2022
S [mm]	6.3	6.3	6.7	7.9	7.8	9.9
V [mm^3]	132	134	157	259	249	505
GLN [-]	1.92	1.60	3.54	2.57	2.70	4.70
WSS_{av} [Pa]	0.32	0.23	0.15	0.12	0.10	0.15
OSI_{av} [-]	0.02	0.02	0.03	0.05	0.06	0.21
$MISES_{av}$ [kPa]	790	800	790	790	930	970

During the initial years of 2012 and 2013 the morphology of the aneurysm did not change considerably, WSS decreased indicating the end of aneurysm initiation and a transition into a dynamic growths period. The mean stress in the wall did not change in this year.

In the next period until 2017 the most significant change occurred in the morphology of the aneurysm. The top right section in figures 1 and 2 of the aneurysm in 2017 shows significant growth in a given direction. This growth not only increases the volume, but also the curvature of the aneurysm. Additional decrease in WSS and a small increase in OSI can be seen, while the wall stress remains constant.

Within a single year until 2018 significant changes can be observed in the behaviour of the aneurysm. The previous growth direction changes and the volume increases significantly by 65% withing one year. WSS decreases and a significant increase in OSI (~77%) can be observed especially in the region of aneurysm growth. This corresponds to findings in [3,16]. Still wall stress remains constant during this strong growth period.

In the next period until 2020 morphology and hemodynamics do not change considerably, however the wall vessel stress increases unexpectedly by ~18% after being constant throughout the previous 6 years. Retrospectively, we know that this event is closest to rupture.

In the last period between 2020 and 2022 SAH occurred in the aneurysm changing the morphology. OSI increases by ~375%, while WSS and Mises stress increase by 49% and 4% respectively.

The evaluation of aneurysm history clearly shows significant events during the years:

1. High WSS region during aneurysm initiation and slow decrease of WSS during aneurysm growth
2. Increase of OSI (especially in the direction of aneurysm growth) over the years.
3. Abrupt changes in geometry induce subsequent changes in hemodynamics implying possible unfavourable growth.
4. Due to increased unfavourable growth wall stress is increased in the years before SAH, while wall stress remains constant beforehand.

5. Conclusion

The evaluation of aneurysm growth history can be a valuable tool in the hands of neurosurgeons. With the help of Fluid-Structure Interaction simulations it is possible to identify the growth history of cerebral aneurysms. By comparing results between patient data taken over the years, significant events can be found in the behaviour of hemodynamics (WSS and OSI), morphology (Size, Volume, GLN) as well as structural mechanics (MISES). Most notably the change in wall stress seems to be closest to aneurysm rupture indicating the most important event in the growth history.

With the ARES Software Suite [13] medical personnel without simulation knowledge can conduct FSI simulations on multiple aneurysms establishing the patient history. Significant changes in morphology, hemodynamics and structural mechanics can indicate certain periods of aneurysm growth and can be used to better estimate the best time for patient treatment.

In future steps, more parameters will be included into evaluation as well as the patient pool will be increased to identify typical events during the growth of cerebral aneurysms.

Acknowledgements

This work was supported by research subsidies granted by the government of Upper Austria via the FFG (Austrian Research Promotion Agency) [grant number 872604 (Project MEDUSA) as well as grant number FO999895610 (Project ARES)]. RISC Software GmbH is Member of UAR (Upper Austrian Research) Innovation Network.

This study was approved by the local ethics committee (Ethikkommission der medizinischen Fakultät der Johannes Kepler Universität; EK Nr: 1129/2022), and the requirement for acquisition of informed consent from patients was waived owing to the retrospective nature of the research.

References

[1] S. Dhar, M. Tremmel, J. Mocco, M. Kim, J. Yamasolo, A . H. Siddiqui, L. N. Hopkins and H. Meng, "Morphology Parameters for Aneurysm Rupture Risk Assessment" *Neurosurgery*, vol. 63, no. 2, pp. 185-197, 2008.

[2] S. Jirjees, Z. M. Htun, I.. Aldawudi, P. C. Patwal and S. Khan, "Role of Morphological and Hemodyanmic Factors in Predicting Intracranial Aneurysm Rutpure: A Review" *Cureus*, vol. 12, no. 7: e9178, 2020.

[3] H. Meng, V.M. Tutino, J. Xiang, and A. Siddiqui: "High WSS or Low WSS? Complex Interactions of Hemodynamics with Intracranial Aneurysm Initiation, Growth, and Rupture: Toward a Unifying Hypothesis" *AJNR Am. J. Neuroradiol.*, vol. 35, no. 7, pp. 1254-1262, 2014.

[4] Japan Investigators UCAS, A. Morita, T. Kirino, K. Hashi, N. Aoki, S. Fukuhara, N. Hashimoto, T. Nakayama, M. Sakai, A. Teramoto, S. Tominari and T. Yoshimoto, "The natural course of unruptured cerebral aneurysms in a Japanese cohort". *N Engl J Med*, vol. 366, pp. 2474- 2482, 2012.

[5] P. Jiang, Q. Liu, J. Wu, X. Chen, M. Li, Z. Li, S. Yang, R. Guo, B. Gao, Y. Cao and S. Wang, "A Novel Scoring System for Rupture Risk Stratification of Intracranial Aneurysms: A Hemodynamic and Morphological Study". *Front. Neurosci*. vol. 12, no. 596, 2018.

[6] F.J. Detmer, B.J. Chung, F. Mut, M. Slawski, F. Hamzei-Sichani, C. Putman, C. Jimenez and J.R. Cebral, "Development and internal validation of an aneurysm rupture probability model based on patient characteristics and aneurysm location, morphology, and hemodynamics". *Int J CARS*, vol. 13, pp. 1767–1779, 2018.

[7] F.J. Detmer, B.J. Chung, F. Mut, M. Slawski, F. Hamzei-Sichani, C. Putman, C. Jimenez and J.R. Cebral, "Development of a statistical model for discrimination of rupture status in posterior communicating artery aneurysms". *Acta Neurochir*, vol. 160, pp. 1643–1652, 2018.

[8] S. Soldozy, P. Norat, M. Elsarrag, A. Chatrath, J.S. Costello, J.D. Sokolowski, P. Tvrdik, M.Y.S. Kalani and M.S. Park. "The biophysical role of hemodynamics in the pathogenesis of cerebral aneurysm formation and rupture". *Neurosurg Focus*. Vol. 47, no. 1, pp. E11. 2019.

[9] J. M. Acosta, A. F. Cayron, N. Dupuy, G. Pelli, B. Foglia, J. Haemmerli, E. Allermann, P. Bijlenga, B. R. Kwak and S. Morel, "Effect of Aneurysm and Patient Characteristics on Intracranial Aneurysm Wall Thickness", *FRONT CARDIOVASC MED*, vol. 8, Article 775307, 2021

[10] J.R. Cebral, F. Mut, D. Sforza, R. Löhner, E. Scrivano, P. Lylyk, C. Putman, "Clinical application of image-based CFD for cerebral aneurysms". *Int. j. numer. method. biomed. eng.*, vol. 27, pp. 977–992, 2011.

[11] T.C. Gasser, M. Auer, F. Labruto, J. Swedenborg, J. Roy, „Biomechanical rupture risk assessment of abdominal aortic aneurysms: Model complexity versus predictability of finite element simulations". *Eur. J. Vasc. Endovasc. Surg.*, vol. 40, pp. 176–185, 2010.

[12] C. Reeps, M. Gee, A. Maier, M. Gurdan, H.H. Eckstein and W.A. Wall, "The impact of model assumptions on results of computational mechanics in abdominal aortic aneurysm", *J. Vasc. Surg.*, vol. 51, pp. 679–688, 2010.

[13] J. Nagy, J. Maier, V. Miron, W. Fenz, Z. Major, A. Gruber and M. Gmeiner, "Methods, Validation and Clinical Implementation of a Simulation Method of Cerebral Aneurysms", *JBEB*, vol. 10, pp. 10-19, 2023, DOI: 10.11159/jbeb.2023.003

[14] H.G. Weller, G. Tabor, H. Jasak, and C. Fureby, "A tensorial approach to computational continuum mechanics using object orientated techniques", *Comput. phys.*, vol. 12, no. 6, pp. 620 – 631, 1998.

[15] P. Cardiff, A. Karač, P. De Jaeger, H. Jasak , J. Nagy, A. Ivanković and Ž. Tuković, "An open-source finite volume toolbox for solid mechanics and fluid-solid interaction simulations", arXiv:1808.10736v2, 2018, Available: https://arxiv.org/abs/1808.10736

[16] S. Fujimura, K. Tanaka, H. Takao, T. Okudaira, H. Koseki, A. Hasebe, T. Suzuki, Y. Uchiyama, T. Ishibashi, K. Otani, K. Karagiozov, K. Fukudome, M. Hayakawa, M. Yamamoto and Y. Murayama, "Computational fluid dynamic analysis of the initiation of cerebral aneurysms", *J Neurosurg*, vol. 137, pp. 335–343, 2022.

[17] P. Blanco, L. Müller and J. David Spence: "Blood pressure gradients in cerebral arteries: a clue to pathogenesis of cerebral small vessel disease", Stroke Vasc. Neurol., vol. 2, no. 3, pp. 108-117, 2017.